Mossbauer and magnetic susceptibility studies on the alloy series $FeAl_{1-x}Cr_x$

Mössbauer and magnetic susceptibility studies on the alloy series FeAl$_{1-x}$Cr$_x$

M A Kobeissi†, Q A Pankhurst, S J Penn and M F Thomas

Department of Physics, University of Liverpool, Liverpool L69 3BX

Abstract. Magnetic susceptibility measurements on the alloy series FeAl$_{1-x}$Cr$_x$ (0.05 ≤ x ≤ 0.60) indicate transitions between paramagnetic and spin glass phases for x = 0.35, x = 0.40 and between paramagnetic and ferromagnetic phases for x = 0.50. Mössbauer experiments show the presence of static magnetic hyperfine interactions for alloys with x ≥ 0.35. The Mössbauer spectra illustrate the spread of electron density and hyperfine magnetic field at the iron sites. The onset of the ferromagnetic phase is explained in terms of the growth of nearest neighbour iron clusters and the critical concentration found for this alloy series 0.4 < x < 0.5 is compared with those observed for the analogous series FeAl$_{1-x}$Cu$_x$ and FeAl$_{1-x}$Fe$_x$.

1. Introduction

This investigation on FeAl$_{1-x}$Cr$_x$ forms part of a set of studies on the magnetism of ternary alloys formed by progressively replacing Al atoms of the ordered alloy FeAl by a transition metal. Former studies dealt with the series FeAl$_{1-x}$Fe$_x$ [1, 2, 3] and FeAl$_{1-x}$Cu$_x$ [4, 5]. The parent alloy Fe–Al crystallizes in the ordered B2 (CsCl) structure and does not show magnetic ordering [1]. However in both FeAl$_{1-x}$Fe$_x$ and FeAl$_{1-x}$Cu$_x$ ferromagnetic and spin glass phases have been observed. In both cases a range of values of x has been discovered for which the ferromagnetic phase is reentrant with a transition from the ferromagnetic to a magnetic glass phase being observed as the temperature is decreased.

It is of interest to explore the mechanisms that lead to ordered phases of FeAl$_{1-x}$T$_x$ as x is increased and to compare the effect of different transition metals T. In these studies the magnetic susceptibility measurements give information on macroscopic properties that identify the magnetic phases and measure the transition temperatures between them. The Mössbauer results give information on the microstructure, in particular the effect of the site by site randomness that occurs as the concentration of the substituting transition metal increases, breaking up the ordered alternation of atoms of the Fe–Al structure. This substitutional behaviour differs between transition metals T. For Fe in FeAl$_{1-x}$Fe$_x$ the excess Fe atoms obviously substitute on the Al sublattice. In FeAl$_{1-x}$Cu$_x$ it has been shown [4] that Cu substitutes randomly on Fe and Al sublattices. In the case of Cr substituting in the series FeAl$_{1-x}$Cr$_x$ the behaviour is more complex.

---

† Present address: Physics Department, UAE University, Al Ain, United Arab Emirates.

In the concentration range $0 < x < 0.2$ the Cr substitutes on the Al sublattice to form the $B2_1$ phase, while increased values $0.2 < x < 0.5$ lead to Cr substituting on both sublattices to give the $B2_3$ phase. At concentrations with $x > 0.5$ the Cr substitutes on the Fe sublattice to give the $B2_2$ phase. In all the substitutions with T = Fe, Cu and Cr, with the exception of the $B2_1$ phase of $FeAl_{1-x}Cr_x$, the net effect is to create nearest neighbour Fe clusters either by adding excess iron as in $FeAl_{1-x}Fe_x$ or by displacing Fe from the Fe to the Al sublattice as in $FeAl_{1-x}Cu_x$ and $FeAl_{1-x}Cr_x$ in the $B2_3$ and $B2_2$ phases. The evidence for these different phases as the Cr concentration x is changed comes from neutron diffraction studies [6]. The Mössbauer results of this study will be seen to be consistent with this picture.

2. Experimental technique

The alloys used in this investigation were those prepared and used in the neutron diffraction and magnetic measurements of Okpalugo *et al* [6].

2.1. Magnetic susceptibility measurements

Samples were prepared by compressing the powdered alloys into nylon holders to form cylinders of 1.5 mm diameter and 20 mm length. The samples were held at the centre of a pickup coil of a previously balanced mutual induction bridge which operated at a frequency of 15 Hz with an RMS field of 8 μT. Static fields of up to 12 mT could be applied parallel to the AC field and to the long axis of the sample. A helium flow cryostat and temperature control system incorporating a resistance thermometer stabilized the temperature to better than 0.5 K in the range 4.2 K to 300 K. Values of magnetic susceptibility χ versus temperature were recorded over a complete up and down temperature cycle starting with the lowest temperature. The temperature of spin glass freezing T_f was taken at the maximum of the cusp of the graphs while the ordering temperature T_C for the paramagnetic to ferromagnetic transition was taken at the point of maximum slope $(d\chi/dT)$ of the graph.

2.2. Mössbauer measurements

The Mössbauer absorbers were made by spreading finely powdered alloys homogeneously on masking tape and enclosing them in polypropylene sample holders. The spectrometers incorporated sources of ^{57}Co in a rhodium matrix driven in double ramp mode. The folded spectra showed a flat background. The spectrometers were calibrated with a thin α-iron foil at room temperature and isomer shift values are quoted relative to these calibrations. Mössbauer transition temperatures T_{hf}, indicated by the detection of a magnetic hyperfine interaction were determined using the thermal scanning method described by Kobeissi [7]. Absorber temperatures were varied using a helium flow cryostat which had temperature stability of better than 0.5 K. The magnetic spectra investigating the distributions of hyperfine field B_{hf} with Cr concentration x were obtained at 4.2 K in a helium bath cryostat.

These spectra were analysed in terms of a probability distribution of correlated isomer shift and hyperfine field represented by an unconstrained histogram. An integrated line shape was used corresponding to the integration of a Lorentzian line over the range of hyperfine fields within each histogram box. Quadrupole splitting was taken
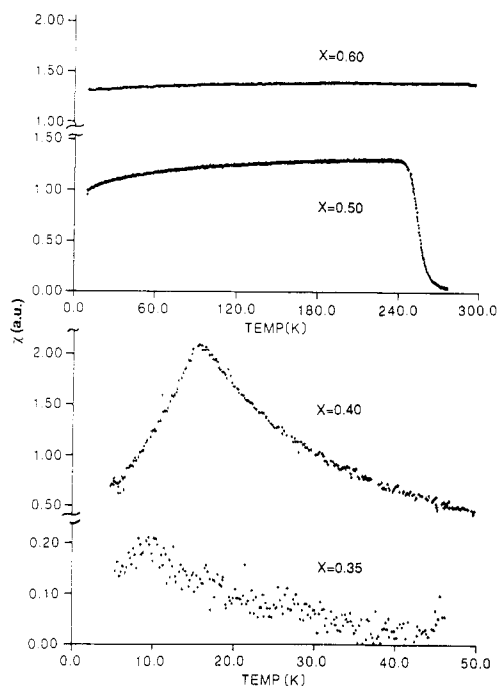
Figure 1. Graphs showing the variation of relative AC susceptibility with temperature for samples with Cr concentrations $x = 0.35$, 0.40, 0.50 and 0.60. For the samples $x = 0.35$ and $x = 0.40$ the graphs illustrate the characteristic cusp that marks the transition between paramagnetic and spin glass phases. The graphs for samples with $x = 0.50$ and $x = 0.60$ illustrate the ferromagnetic phase with a transition to the paramagnetic phase in the case of $x = 0.50$.
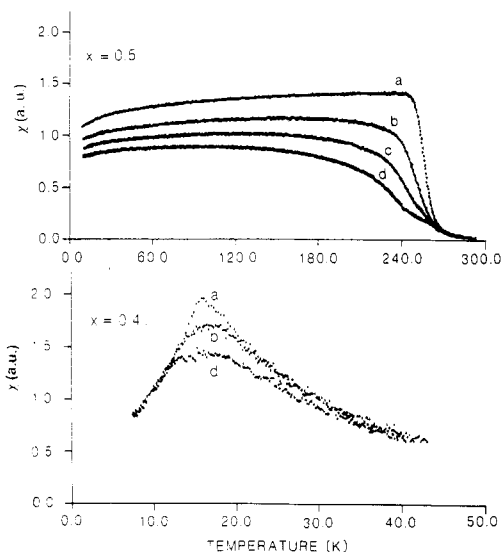
Figure 2. Graphs of relative AC magnetic susceptibility versus temperature for samples with $x = 0.40$ and 0.50 in DC fields of (*a*) zero, (*b*) 4 mT, (*c*) 8 mT and (*d*) 12 mT.

to be negligible and a linear correlation between increasing isomer shift and decreasing hyperfine field was assumed. This correlation agrees with the observed behaviour of the mean values $\bar{\delta}$ and $\bar{B}_{\mathrm{hf}}$ as x is varied and is in line with the picture of electron occupation of the 3d shell in the iron atoms that is discussed below.

3. Results

3.1. Measurements of AC susceptibility χ_{AC}

The range of samples of FeAl$_{1-x}$Cr$_x$ comprised values of $x = 0.05, 0.10, 0.15, 0.20, 0.30,$ $0.35, 0.40, 0.50$ and 0.60 but for alloys with $x < 0.25$ the values of susceptibility were too small to be reliably measured. Graphs of the variation of χ_{AC} with temperature for the samples with $x \geqslant 0.35$, are shown in figure 1. It is seen that these graphs fall into two types. The samples with $x = 0.35$ and $x = 0.40$ give graphs that show cusps at well defined temperatures characteristic of a transition between paramagnetic and spin glass phases [8, 9]. The temperature of the transition T_f corresponds to the fluctuations of the iron

Table 1. The first column shows the Cr concentration x in the alloy series $FeAl_{1-x}Cr_x$, the second column lists the mean isomer shifts at 300 K taken as the centre of gravity of the broadened single line with respect to iron metal. The third column is the mean hyperfine field at 4.2 K taken as the centre of gravity of the $P(B_{hf})$ distribution. The values of hyperfine temperature in column four are the highest temperatures at which magnetic broadening of the spectra are observed. The Curie temperature T_C and the freezing temperature T_f shown in columns five and six are taken from the susceptibility versus temperature graphs of figure 1.

Cr content, x	Mean isomer shift, $\bar{\delta}$ (mm s^{-1})	Mean hyperfine field, $\bar{B}_{hf}$ (T)	Hyperfine temperature, T_{hf} (K)	Curie temperature, T_C (K)	Freezing temperature, T_f (K)
0.05	0.243 ± 0.005				
0.10	0.223				
0.15	0.206				
0.20	0.165				
0.30	0.150	3.4			
0.35	0.136	5.5	10 ± 1		9 ± 1
0.40	0.123	7.6	23 ± 1		16 ± 1
0.50	0.086	12.1	250 ± 3	253 ± 3	<5
0.60		15.8	413 ± 3	>300	<5

magnetic moments in the paramagnetic phase freezing into static orientations in the spin glass phase. The freezing temperatures T_f increase with Cr content x; values of T_f are listed in table 1. For the sample with $x = 0.50$ a sharp rise in χ_{AC} is observed as the temperature is decreased, characteristic of a transition from the paramagnetic to the ferromagnetic phase. The temperature of this ordering transition T_C, taken at the point of maximum $(d\chi/dT)$ is listed in table 1. In the ferromagnetic phase the large susceptibility response is limited by the demagnetization factor [2]. At the lowest temperatures a decrease in susceptibility is seen which, by analogy with similar results for $FeAl_{1-x}Cu_x$ [5], may herald a phase transition to the spin glass phase at temperatures $T_f < 6$ K. The graph of the $x = 0.60$ sample is interpreted as being in the ferromagnetic phase throughout, thus setting limits of $T_C > 300$ K and possibly $T_f < 5$ K.

The effect of static applied fields on the graphs of χ_{AC} versus temperature for the samples with $x = 0.40$ and $x = 0.50$ are shown in figure 2. For the $x = 0.40$ sample fields of 4 mT and 12 mT progressively smear out the cusp to produce a rounded maximum which is typical behaviour for a transition between paramagnetic and spin glass phases [8]. For the sample with $x = 0.50$ applied fields of 4 mT, 8 mT and 12 mT progressively decrease the value of χ_{AC} by suppressing domain movement [9].

3.2. Mössbauer spectra

The spectra of samples with x up to 0.50 taken at 300 K, are shown in figure 3 and are seen to consist of a single line broadened above the instrumental value of 0.26 mm s^{-1} (the sample with $x = 0.60$ showed magnetic hyperfine interactions in agreement with the susceptibility results). The values of full width at half maximum for the single line spectra increase from 0.45 mm s^{-1} for the $x = 0.05$ sample to 0.55 mm s^{-1} for the $x = 0.50$ sample. These single lines have asymmetric profiles interpreted as reflecting
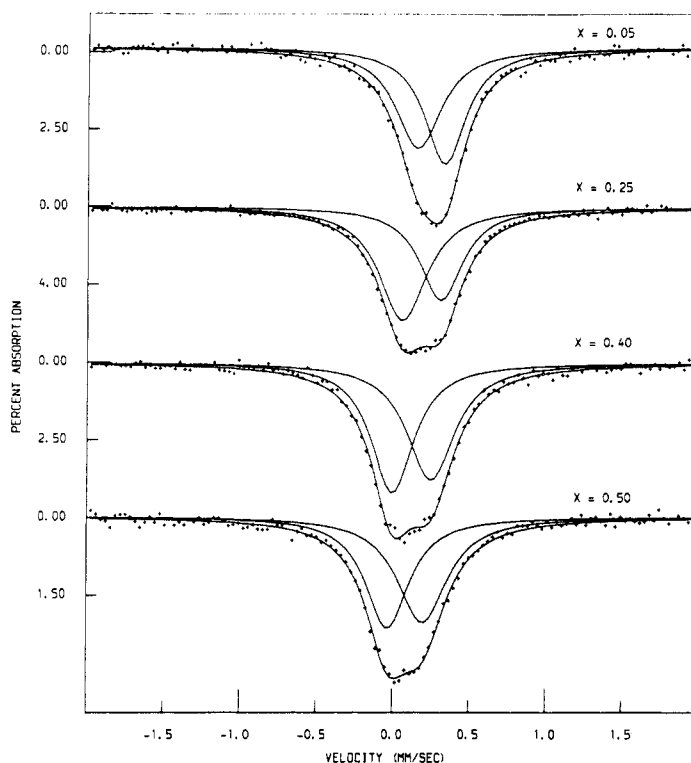
Figure 3. Mössbauer spectra of samples with $x \leqslant 0.50$ taken at 300 K. The spectra can be fitted satisfactorily with two single lines which enables values of the mean isomer shift to be obtained from weighted averages of these lines.

the distribution in electron density at Fe sites surrounded by different combinations of neighbouring atoms. The mean velocity value of the centroid of the line $\bar{\delta}$ for each sample was extracted and values of $\bar{\delta}$ accurate to ~ 0.005 mm s^{-1} are listed in table 1. It is seen in the plot of $\bar{\delta}$ versus x shown in figure 4 that $\bar{\delta}$ decreases steadily as x increases. Figure 4 also shows that the rate of decrease of $\bar{\delta}$ with x is slightly greater for $0.05 < x < 0.20$ than for $0.25 < x < 0.50$, and that the point for $x = 0.50$ lies significantly low. We believe it is significant that the values of x that show discontinuities in the $\bar{\delta}$ versus x plot correspond with the $B2_1 \rightarrow B2_3 \rightarrow B2_2$ phase changes observed by neutron diffraction. Complexities in fitting the magnetic spectrum for the $x = 0.60$ sample made its value insufficiently precise to be included in this trend. The overall decrease in $\bar{\delta}$ with x is similar to that observed in $FeAl_{1-x}Cu_x$ [5] and is, we believe, attributable to the same cause whereby with increasing x the population of the 3d electrons around the Fe atom decreases reducing the shielding of the s shell electrons. The increased s electron density at the Fe nucleus as x increases produces the decrease in the isomer shift value $\bar{\delta}$. It is noticable in figure 4 that the difference in the slope of the $\bar{\delta}$ versus x variation above and below the value $x = 0.20$ matches the change in structure from $B2_1$ to $B2_3$ observed at $x = 0.20$ by Okpalugo *et al* [6].

At 4.2 K the spectra of the alloys with $x \geqslant 0.30$ showed additional magnetic broadening. These spectra are shown in figure 5 where it can be seen that the magnetic
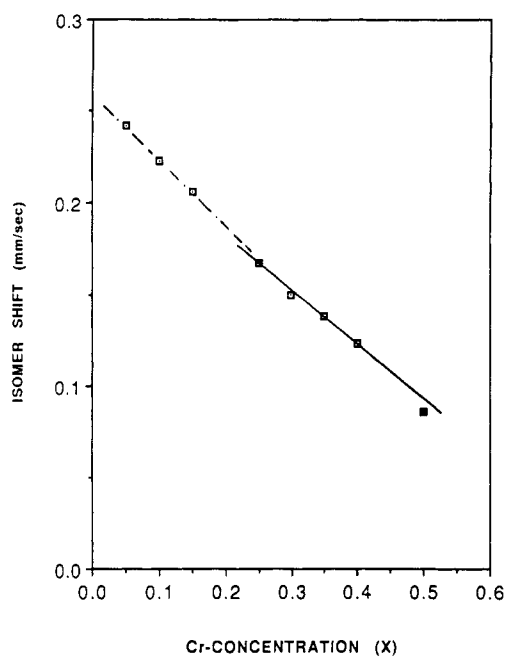
Figure 4. Variation of mean isomer shifts $\bar{\delta}$ with Cr concentration x taken from the data of figure 3.
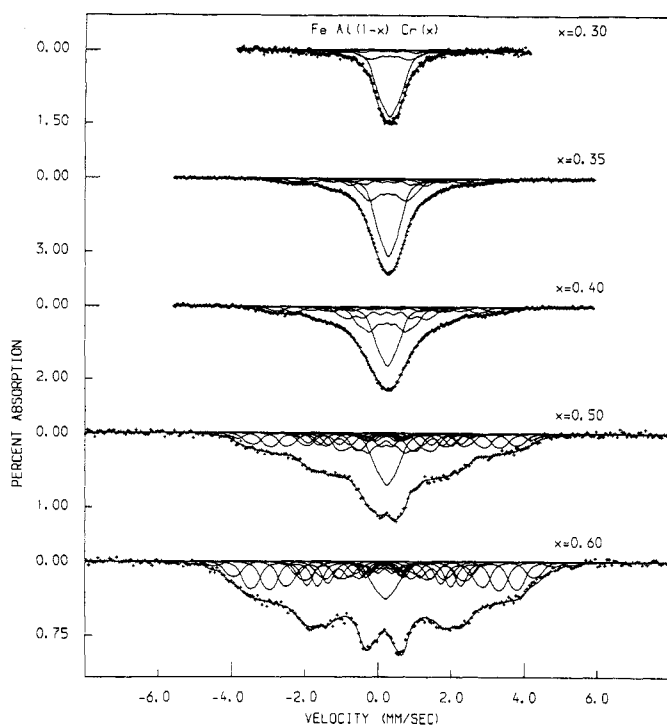

Figure 5. Mössbauer spectra taken at 4.2 K for samples with $x \geq 0.30$. Fits to the spectra are generated from the distribution of hyperfine fields shown in figure 6.
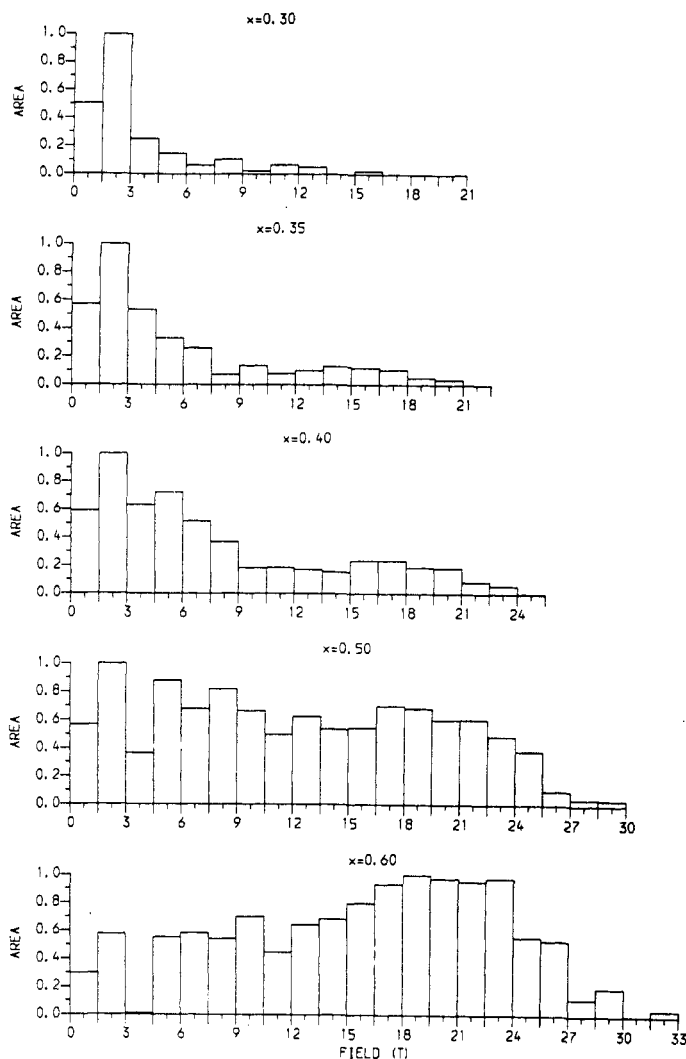
Figure 6. Probability distributions of hyperfine field $P(B_{hf})$ derived from the spectra of figure 5 by a fitting program that superposes spectral components with hyperfine field and intensity given by each hyperfine field bin.

broadening increases with increasing x. The broad features of these spectra, reflecting the spread of different local environments around the Fe nuclei, were fitted by distributions of hyperfine fields. The histograms of hyperfine fields, derived from fits to the spectra of figure 5, are shown in figure 6. The mean value of the hyperfine field $\bar{B}_{hf}$ is evaluated from each histogram and is listed in table 1 where it is seen that $\bar{B}_{hf}$ increases steadily with x. The correlation between increased hyperfine field and decreased isomer shift incorporated in the fits is implicit in the model whereby decreasing 3d population on the iron atom causes increased s electron density at the nucleus. In such a system increased $\bar{B}_{hf}$ and decreased $\bar{\delta}$ are correlated provided that the iron 3d shell is more than half filled so that decreasing 3d population increases the mean $\langle S \rangle$ of the atom by removing electrons with spins antiparallel to the majority direction.
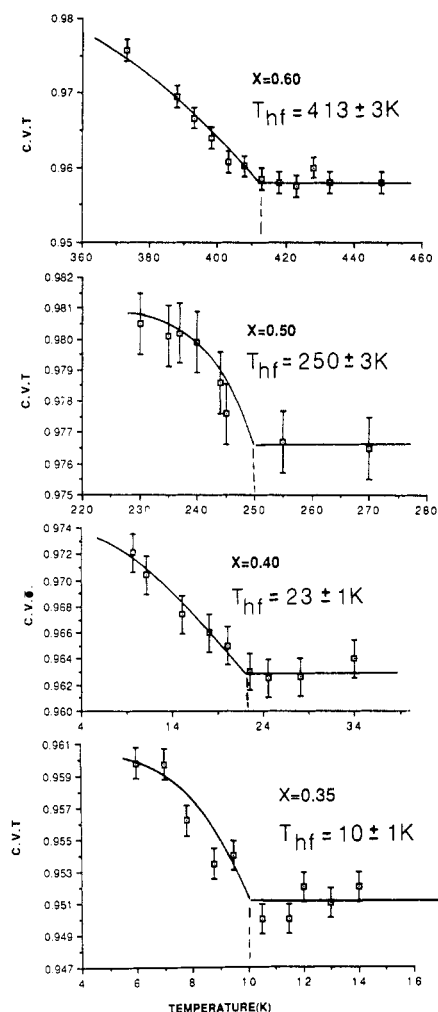
Figure 7. Determination of hyperfine temperatures T_{hf} by plotting the centroid velocity transmission versus temperature for samples with $x = 0.35, 0.40, 0.50$ and 0.60.

The temperatures T_{hf} at which the Mössbauer spectra exhibited magnetic splitting were determined from the graphs of centroid velocity transmission versus temperature shown in figure 7. Centroid velocity transmission is defined here as the ratio of counts in the channel of maximum absorption to those in a background channel where there is no resonant absorption. The onset of magnetic hyperfine interaction denotes a hyperfine field at the iron nuclei which is static or varies slowly compared to the Mössbauer measuring time of $\sim 10^{-7}$ s. Values of T_{hf} determined in this way are listed in table 1.

4. Discussion

The magnetic susceptibility results of figure 1 and the Mössbauer determinations of T_{hf} shown in figure 7 are used to construct the phase diagram shown in figure 8. The
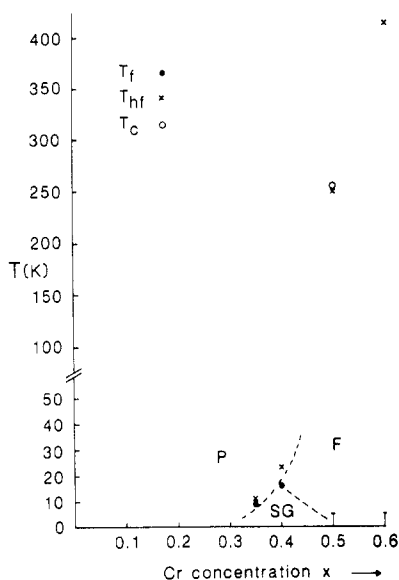
Figure 8. Plot of T_f, T_C and T_{hf} versus Cr concentration x which enables a magnetic phase diagram for the series of alloys to be indicated by dashed lines. *P*, *F* and *SG* denote paramagnetic and spin glass phases respectively.

possibility that the decrease in susceptibility at the lowest temperature for the samples with $x = 0.50$ and 0.60 may herald a transition from the ferromagnetic to the spin glass phase similar to that observed in the alloy FeAl$_{0.675}$Cu$_{0.325}$ is denoted by the limits for $T_f < 5$ K indicated for these compositions. Mössbauer spectra taken at 4.2 K for these alloys do not distinguish between ferromagnetic and spin glass phases. The distribution of hyperfine fields observed in these spectra reflect the many different combinations of nearest neighbour atoms around the iron sites. This multiplicity of short range conditions will produce the observed spread of hyperfine fields in either a ferromagnetic or a spin glass phase.

The results illustrated in figure 8 establish a magnetic phase diagram with paramagnetic, ferromagnetic and spin glass regions. The ferromagnetic phase arises for a Cr content of $0.4 < x < 0.5$. Similar studies on the series FeAl$_{1-x}$Cu$_x$ [5] determine that the ferromagnetic phase occurs for a Cu concentration of $0.25 < x < 0.325$ while in FeAl$_{1-x}$Fe$_x$ a ferromagnetic phase is observed for $x = 0.10$ [1] setting the limit at $x < 0.1$ for this series. Thus in order to produce a ferromagnetic phase progressively larger amounts of transition metal T are required as T changes from Fe to Cu to Cr.

In attempting to account for these results the effects of lattice dimensions and conduction electron density may play a part but we believe that the strongest single influence in the formation of the ferromagnetic phase comes from the action of the substituting transition metal T in forming the nearest neighbour iron clusters. The parent alloy of all the ternary series is the binary alloy Fe–Al which crystallizes in the ordered B2 (CsCl) structure. For the series FeAl$_{1-x}$Fe$_x$ each Fe atom corresponding to $x > 0$ can be regarded as displacing an Al atom of the B2 structure and thus such an Fe atom has eight Fe nearest neighbours. In this substitution the nearest neighbour clusters build up most quickly as x is increased. In the series FeAl$_{1-x}$Cu$_x$ it has been shown [4] that the

Cu atoms substitute randomly on the Fe and Al sublattices of the ordered Fe–Al. The substitution of Cu on the Al sublattice creates no iron nearest neighbour clusters but substitutions on the Fe sublattice results in a displaced Fe atom occupying a site on the Al sublattice with Fe nearest neighbours to promote the iron clustering. This mechanism, incorporating the random substitution of Cu on the Fe and Al sublattices, implies that Cu substitution should be approximately half as effective as Fe substitution in forming iron nearest neighbour clusters. In the series $FeAl_{1-x}Cr_x$ it has been shown [6] that for $x < 0.2$ the Cr substitutes only on the Al sublattice (the $B2_1$ structure) and for values of $0.2 < x < 0.5$ substitutes on both sublattices (the $B2_3$ structure). At each level of Cr concentration x the preference of Cr substitution on the Al sublattice causes less Fe displacement and consequently less iron cluster formation than occurs for Cu substitution. Thus the effectiveness of a level x of substitution of transition metal T in promoting the ferromagnetic phase through formation of iron nearest neighbour clusters increases as T changes from Cr to Cu to Fe.

In the case of the $FeAl_{1-x}Cu_x$ series of alloys a simulation calculation showed [5] that it was likely that a percolating cluster of nearest neighbour iron atoms was formed at a copper concentration of $x \sim 0.24$, close to the observed critical concentration. Similar calculations are more problematic in the case of the Cr series since the assumption of random substitution on Fe and Al sublattices cannot be made but we believe that the qualitative argument above shows that the largest factor in the establishment of a ferromagnetic phase is the efficiency with which the substituting transition metal T forms iron atom clusters.

The Mössbauer spectra give information on the microscopic environment surrounding the iron atoms. The broadened singlet spectra observed at room temperature and the 4.2 K spectra broadened by a range of hyperfine fields show that randomness caused by the substitution of Cr for Al atoms results in distributions of isomer shift δ and hyperfine field B_{hf}. Mean values of δ, listed in table 1 and shown in figure 4 show a somewhat sharper decline with increasing x for values of $x < 0.2$ where Cr substitutes only on the Al sublattice than for $x > 0.2$ when the Cr substitutes on both Al and Fe sublattices. The hyperfine field distributions of figure 6 are also due to the range of near neighbour environments. It is well known from studies on binary alloys containing iron [10] that the hyperfine field on an iron atom is affected by its nearest neighbour atoms, presumably through local changes in the polarization of conduction electrons. In discussing magnetic measurements on the $FeAl_{1-x}T_x$ alloys Okpalugo *et al* [6] compare these alloys to the similar series of $CoGa_{1-x}Co_x$ alloys where neutron diffraction studies showed that the magnetic moments of Co atoms displaced onto the Ga sites were an order of magnitude greater than those of Co atoms on their original sublattice. If similar behaviour were occurring in the $FeAl_{1-x}Cr_x$ series it would show up in the $P(B_{hf})$ distributions of figure 6. The results in this study and a former study on $Fe\,Al_{1-x}Cu_x$ [5] shows that as x increases the mean moment on the iron atoms increases but in both series the distributions appear to be due to a wide variety of local environments rather than two quasi discrete sets of moments corresponding to iron atoms on the two sublattices. The $P(B_{hf})$ distributions give no direct evidence on any moment on the Cr atoms or whether, as in the case of **FeCr**, such Cr moments are ordered antiferromagnetically with respect to the iron magnetization.

Comparison of the freezing temperature T_f and the hyperfine field temperature T_{hf} for the alloys $x = 0.35$ and $x = 0.40$ corresponding to the transition temperature between paramagnetic and spin glass phases measured by magnetic susceptibility and Mössbauer spectroscopy respectively show that $T_{hf} > T_f$. This reflects the fact that the temperature

at which magnetic fluctuations become slower than the Mössbauer measuring time of $\sim10^{-7}$ s is higher than the freezing temperatures measured on the AC susceptibility timescale of $\sim10^{-1}$ s.

Acknowledgments

References

[1] Wertheim G K and Wernick J H 1967 *Acta Metallurgica* **15** 297–302
[2] Shull R D, Okamoto H and Beck P A 1976 *Solid State Commun.* **20** 863–8
[3] Chachem H, Galvao de Silva E, Guenzburger D and Ellis D E 1987 *Phys. Rev.* B **35** 1602–8
[4] Saleh A S, Mankikar R M, Yoon S, Okpalugo D E and Booth J G 1985 *J. Appl. Phys.* **57** 3421–3
[5] Kobeissi M A, Pankhurst Q A, Suharan S and Thomas M F 1990 *J. Phys.: Condens. Matter* **2** 4895–906
[6] Okpalugo D E, Booth J G and Faunce C A 1985 *J. Phys. F: Met. Phys.* **15** 681–92
[7] Kobeissi M A 1981 *Phys. Rev.* B **24** 2380–96
[8] Moorjani K and Coey J M 1984 *Magnetic Glasses* (Amsterdam: Elsevier) p 329
[9] Huang C Y 1985 *J. Magn. Magn. Mater.* **51** 1–74
[10] Johnson C E, Ridout M S and Cranshaw T E 1963 *Proc. Phys. Soc.* **81** 1079–90